Solving coupled equations by iteration for heavy ion multiple Coulomb excitation

L. D. Tolsma
Department of Physics, Eindhoven University of Technology, Eindhoven, The Netherlands
(Received 26 December 1978)

The set of coupled linear second-order differential equations which has to be solved for quantum-mechanical calculations of inelastic scattering processes with multiple excitation can be rewritten as an equivalent set of coupled first-order integral equations. When Airy functions are used as piecewise analytic reference solutions, it makes it possible to evaluate analytically the integrals that arise in the set of integral equations. This set can be solved iteratively with a considerable reduction of computation time in cases of heavy ion scattering, when compared to quantum-mechanical coupled-channel calculations of the conventional type. The efficiency of two iteration schemes, an inward-outward and a perturbative one, has been investigated for some test cases dealing with multiple Coulomb excitation of ^{238}U by Kr and Pb. It turns out that, for heavy ion scattering, only the inward-outward iteration scheme has a practical importance. Finally, the excitation probabilities for ^{238}U, Coulomb excited by 385 MeV Kr up to $I = 24\hbar$, are shown for a reduced $E2$ transition matrix element of 3.5 eb and they are compared with the excitation probabilities calculated according to the semiclassical theory.

[NUCLEAR REACTIONS Solving coupled equations by iteration; quantum mechanically calculated excitation probabilities for heavy ion multiple Coulomb excitation.]

I. INTRODUCTION

For collisions between heavy ions, the asymptotic de Broglie wavelength associated with the relative motion is very short as compared to the long range of the strong Coulomb interaction. In general also many open channels are involved to a significant extent. In heavy ion multiple Coulomb excitation, the rotational bands of a deformed target nucleus can be excited up to $I \gtrsim 20\hbar$. The analysis of such excitations can be performed according to the semiclassical theory, in which the influence of the energy transfer and the change in orbital angular momentum during the collision are neglected in principle.[1] However, for an accurate analysis of the excitations of the high-spin states, or a study of the deviations with respect to semiclassical theories in more general circumstances,[2] it is advisable to have the disposal of fully quantum-mechanical calculations of the cross sections. These coupled-channel calculations of conventional type are not feasible yet, due to the tremendous amount of computation time needed. An attempt has been made to find a solution to this problem by investigating the application of a method for solving systems of coupled linear second-order differential equations by iteration.

The efficiency of this method, as in Gordon's method,[3] depends upon the possibility to divide the integration range into intervals which are sufficiently small to approximate the potential by some more simply varying reference potential but which, on the other hand, contains a sufficiently large number of de Broglie wavelengths. For heavy ion collisions, both conditions are fulfilled. A further element of the method is the decomposition of the partial wave radial solution into regular and outgoing components. This means that the solution in, e.g., the classically allowed region is written as a linear combination of two rapidly oscillating base functions with more or less slowly varying amplitudes. The chosen reference potential allows these base functions to be expressed in terms of piecewise analytic reference solutions. Taking the reference potential over the interval as a linear one, these reference solutions are given by Airy functions.[3]

The Schrödinger equation for the partial wave radial solution is rewritten in an integral form which leads to a system of coupled first-order integral equations for the amplitudes. These amplitudes are obtained by means of an iteration procedure. Two iteration schemes, an inward-outward[4,5] and a perturbative one,[6] have been investigated. When compared to previous applications of these iteration schemes, the advantage of the new method is that the integrals are evaluated analytically.

Although the results are presented for some Coulomb excitation inelastic scattering problems, it is possible in principle to include the influence of a nuclear interaction. Inelastic heavy ion scattering cases involving an optical potential are now being investigated.

In the next section, a concise formulation is given for the quantum-mechanical theory of in-

elastic scattering as applied to multiple Coulomb excitation. In Sec. III, the calculation procedure is discussed and the two iteration schemes are described. In Sec. IV the results of the study that considers the above-mentioned amplitudes is presented, plus the scattering matrix elements for the heavy ion multiple Coulomb excitation of ^{238}U by 385 MeV Kr and 1000 MeV Pb. Both iteration schemes are illustrated by figures and a table which show the rate of convergence and the accuracy achieved. In Sec. V, the excitation probabilities for ^{238}U, Coulomb excited by 385 MeV Kr up to $I=24\hbar$, is shown for a reduced $E2$ transition matrix element of 3.5 eb and is compared with results from the semiclassical theory with energy-symmetrized classical orbits.[1] In the last section some conclusions are drawn.

II. CONCISE QUANTUM-MECHANICAL FORMULATION OF INELASTIC SCATTERING

In general, the quantum-mechanical description of inelastic scattering leads to a set of coupled second-order differential equations of the partial wave radial functions ψ^J_{Il} of the following form:

$$\left[\frac{d^2}{dr^2}+k_I{}^2-\frac{2\eta_I k_I}{r}-\frac{l(l+1)}{r^2}\right]\psi^J_{Il}(r)=\sum_{I'l'}V^J_{Il;I'l'}(r)\,\psi^J_{I'l'}(r), \quad (2.1)$$

for a spinless projectile. Here J, l, and I denote the total angular momentum, the orbital angular momentum, and the spin of the target nucleus with excitation energy ϵ_I, respectively. The total angular momentum J, its projection on the z axis and the parity are good quantum numbers. The wave number k_I and Sommerfeld parameter η_I are given by

$$k_I{}^2=\frac{2\mu}{\hbar^2}(E-\epsilon_I), \qquad \eta_I=\frac{2\mu}{\hbar^2}\frac{Z_1Z_2e^2}{2k_I}, \quad (2.2)$$

where μ is the reduced mass, while Z_1 and Z_2 represent the charge numbers of the projectile and target nucleus, respectively. The coupling potential for the special case of multiple Coulomb excitation is given by[7]

$$V^J_{Il;I'l'}(r)=\frac{2\mu}{\hbar^2}Z_1e\sqrt{4\pi}\sum_\lambda\left(\frac{(2l+1)(2l'+1)}{2\lambda+1}\right)^{1/2}(-1)^{J+I'+\lambda}\langle I'\|M(E\lambda)\|I\rangle\begin{pmatrix}l & l' & \lambda\\ 0 & 0 & 0\end{pmatrix}\begin{Bmatrix}J & l' & I'\\ \lambda & I & l\end{Bmatrix}\frac{1}{r^{\lambda+1}}, \quad (2.3)$$

where $\langle I'\|M(E\lambda)\|I\rangle$ denotes the reduced matrix element of the electric 2^λ-pole moment of the target.

To obtain the solutions for $\psi^J_{Il}(r)$, two boundary conditions have to be fulfilled. At the origin, they must vanish and for large distances they must be related to an ingoing partial wave in the entrance channel plus outgoing partial waves in all relevant exit channels. The precise asymptotic form defines a scattering matrix. We follow Alder and Winther's convention[7] for defining an R matrix by the following asymptotic condition:

$$\psi^{J(I_0l_0)}_{Il}\underset{r\to\infty}{\sim}H^-_l(\eta_I;k_Ir)\,\delta_{II_0}\delta_{ll_0}-\left[\frac{k_{I_0}}{k_I}\right]^{1/2}R^J_{Il;I_0l_0}H^+_l(\eta_I;k_Ir). \quad (2.4)$$

The ingoing and outgoing Coulomb waves H^-_l and H^+_l, respectively, are given by $H^\pm_l=(G_l\pm iF_l)$, in terms of the well-known regular and irregular Coulomb wave functions F_l and G_l. The indices I_0, l_0 correspond to an ingoing wave in the entrance channel for $I=I_0$ and $l=l_0$.

The dimension N of the set (2.1) is determined largely by the maximum value $I_{\max}$ of the target spin. Considering the excitation of a ground state rotational band with spin sequence $0^+, 2^+, 4^+, \ldots, I_{\max}$, N is given by

$$N=\sum(I_n+1). \quad (2.5)$$

This means that for $I_{\max}=20$, N becomes 121 and for even higher values of $I_{\max}$, N assumes huge values. In conventional coupled-channel calculations, the set (2.1) has to be solved N times for each J value in order to satisfy the boundary conditions. Especially for large systems this is time consuming. In addition, this procedure generates R-matrix elements which form a complete $N\times N$ matrix. However, in the nuclear physics context of a case with a zero-spin ground state, only one column of this matrix is needed, namely those elements which connect the ground state entrance channel to all the experimentally relevant exit channels. This is the motivation to study iteration methods for which the solutions $\psi^J_{Il}(r)$ are obtained directly without the need for solving the set (2.1) N times.

The scattering amplitudes are expressed in terms of the R-matrix elements[7]

$$f(\theta,\phi)_{I_0M_0\to IM}=\frac{\sqrt{4\pi}}{(k_{I_0}k_I)^{1/2}}\sum_{l_0lJ}(2l_0+1)^{1/2}i^{l_0-l}\langle l_0 0 I_0M_0|JM_0\rangle\langle lmIM|JM_0\rangle$$
$$\times\frac{1}{2i}\{\exp[i(\sigma_{l_0}+\sigma_l)]R^J_{Il;I_0l_0}-\delta_{II_0}\delta_{ll_0}\}Y_{lm}(\theta,\phi), \tag{2.6}$$

in which σ_l is the Coulomb phase shift

$$\sigma_l(\eta)=\arg\Gamma(l+1+i\eta). \tag{2.7}$$

From the scattering amplitudes it is easy to calculate the cross section for state I

$$\frac{d\sigma_I(\theta)}{d\Omega}=\frac{1}{2I_0+1}\frac{k_I}{k_{I_0}}\sum_{M_0M}|f_{I_0M_0\to IM}(\theta,\phi=0)|^2 \tag{2.8}$$

and other observable quantities. The excitation probability, for instance, is given by[8]

$$P_I(\theta)=\frac{k_I}{k_{I_0}}\frac{d\sigma_I}{d\sigma_R}, \tag{2.9}$$

where σ_R is the Rutherford cross section.

III. THE CALCULATION PROCEDURE

The Schrödinger equation (2.1) is rewritten in the more convenient form

$$\left[\frac{d^2}{dr^2}+k_i^2-U_{ii}(r)\right]\psi_i(r)=\sum_{j\neq i}^{N}U_{ij}(r)\psi_j(r),\quad i=1,2,\ldots,N \tag{3.1}$$

and the boundary condition (2.4) as

$$\psi_i^k(r)\underset{r\to\infty}{\sim}\delta_{ik}H_i^- -\left[\frac{k_k}{k_i}\right]^{1/2}R_{ik}H_i^+. \tag{3.2}$$

The superscript and subscript k denotes the entrance channel.

When considering some interval of the integration range with its midpoint at radius $\bar{r}$ and expanding the potential function in a Taylor series, the equation is the following:

$$\left[\frac{d^2}{dr^2}+k_i^2-\sum_{m=0}^{2}\frac{(r-\bar{r})^m}{m!}\frac{d^mU_{ii}(r)}{dr^m}\bigg|_{r=\bar{r}}\right]\psi_i(r)=\sum_{j\neq i}^{N}\left[\sum_{m=0}^{2}\frac{(r-\bar{r})^m}{m!}\frac{d^mU_{ij}(r)}{dr^m}\bigg|_{r=\bar{r}}\right]\psi_j(r). \tag{3.3}$$

Subsequently, introducing an average value for the components of the first derivatives at the left-hand side,

$$\left[\frac{d^2}{dr^2}+k_i^2-U_{ii}(\bar{r})-(r-\bar{r})\frac{dU_{\mathrm{av}}(r)}{dr}\bigg|_{r=\bar{r}}\right]\psi_i(r)$$
$$=\left\{(r-\bar{r})\left[\frac{dU_{ii}(r)}{dr}\bigg|_{r=\bar{r}}-\frac{dU_{\mathrm{av}}(r)}{dr}\bigg|_{r=\bar{r}}\right]+\frac{(r-\bar{r})^2}{2}\frac{d^2U_{ii}(r)}{dr^2}\bigg|_{r=\bar{r}}\right\}\psi_i(r)$$
$$+\sum_{j\neq i}^{N}\left[\sum_{m=0}^{2}\frac{(r-\bar{r})^m}{m!}\frac{d^mU_{ij}(r)}{dr^m}\bigg|_{r=\bar{r}}\right]\psi_j(r) \tag{3.4}$$

or, in more convenient notation,

$$\left[\frac{d^2}{dr^2}+k_i^2-\bar{U}_{ii}(\bar{r})-(r-\bar{r})\frac{dU_{\mathrm{av}}(r)}{dr}\bigg|_{r=\bar{r}}\right]\psi_i(r)=\sum_{j}^{N}W_{ij}(r)\psi_j(r), \tag{3.5}$$

where $\bar{U}_{ii}$ is introduced as the average value of the diagonal potential for the interval. The potential form at the left-hand side is the reference potential. The reason for introducing an average value of the first derivatives will become clear later in this paper.

If the right-hand side of Eq. (3.5) is replaced by zero, each of the resulting decoupled equations has two linearly independent solutions:

1. The regular solution $G_i(r)$. It is defined to vanish at the origin and by the asymptotic form

$$G_i(r) \underset{r\to\infty}{\sim} \frac{i}{2\sqrt{k_i}}[H_i^-(\eta_i; k_i r) - R_i^0 H_i^+(\eta_i; k_i r)] . \tag{3.6a}$$

2. The irregular outgoing wave solution $G_i^+(r)$. This is defined by the asymptotic form

$$G_i^+(r) \underset{r\to\infty}{\sim} \frac{1}{\sqrt{k_i}} H_i^+(\eta_i; k_i r) . \tag{3.6b}$$

Owing to the special form of the left-hand side of Eq. (3.5), the solutions (3.6) can be expressed in terms of Airy functions which can be efficiently evaluated numerically, as shown by Gordon[3]

$$G_i(r) = \mathrm{Ai}[\alpha(\beta_i + r)]\, a_i + \mathrm{Bi}[\alpha(\beta_i + r)]\, b_i \tag{3.7a}$$

and

$$G_i^+(r) = \mathrm{Ai}[\alpha(\beta_i + r)]\, a_i^+ + \mathrm{Bi}[\alpha(\beta_i + r)]\, b_i^+ , \tag{3.7b}$$

with the constants

$$\alpha = \left(\frac{dU_{\mathrm{av}}(r)}{dr}\bigg|_{r=\bar{r}}\right)^{1/3} ,$$
$$\beta_i = \frac{\bar{U}_{ii}(\bar{r}) - k_i^2}{dU_{\mathrm{av}}(r)/dr\,|_{r=\bar{r}}} - \bar{r} . \tag{3.8}$$

The constant coefficients a_i, b_i and a_i^+, b_i^+ are determined by conditions of continuity at the interval boundaries.

Now the Green's function which belongs to the coupled differential Eq. (3.5) can be introduced; it is regular at the origin and has an outgoing wave asymptotic form of

$$G_i(r, r') = -G_i(r_<)\, G_i^+(r_>) . \tag{3.9}$$

where $r_<$ and $r_>$ are the smaller and the larger values of r and r', respectively.

With an ingoing wave in the entrance channel k, the coupled differential Eq. (3.5) can be written as a set of N coupled integral equations

$$\psi_i^k(r) = G_i(r)\left[\frac{2}{i}\delta_{ik} - \int_r^\infty G_i^+(r') \sum_{j=1}^N W_{ij}(r')\,\psi_j^k(r')\,dr'\right] - G_i^+(r)\left[\int_0^r G_i(r') \sum_{j=1}^N W_{ij}(r')\,\psi_j^k(r')\,dr'\right] . \tag{3.10a}$$

Equivalently,

$$\psi_i^k(r) \equiv G_i(r)\, c_i(r) - G_i^+(r)\, c_i^+(r) , \tag{3.10b}$$

with the boundary conditions

$$c_i(\infty) = \frac{2}{i}\delta_{ik} \tag{3.11a}$$

and

$$c_i^+(0) = 0 . \tag{3.11b}$$

In practice, however, instead of Eq. (3.11b) the approximate condition

$$c_i^+(r_0) = \int_0^{r_0} G_i(r') \sum_{j=1}^N W_{ij}(r')\,\psi_j^k(r')\,dr' = 0 \tag{3.11c}$$

is used for a relatively small r_0, in order to prevent the set of integral equations becoming singular.

The choice of r_0 is very important. It must be neither too small nor too large. Of course, the R-matrix elements have to be independent of the actual value of r_0. In Sec. IV this subtle point is discussed in more detail. The asymptotic value of the outgoing coefficients $c_i^+(r)$ are related to the R-matrix elements

$$c_i^+(\infty) = R_{ik} - R_i^0\,\delta_{ik} . \tag{3.12}$$

The set of coupled integral equations (3.10) can be solved by iteration. We have concentrated our investigation on the behavior of the amplitudes $c_i(r)$ and $c_i^+(r)$ instead of the wave function itself. This has been done for two iteration schemes.

A. Inward-outward iteration scheme

In this scheme, the following set of coupled integral equations for the amplitudes $c_i(r)$ and $c_i^+(r)$ are considered:

$$c_i(r) = \frac{2}{i}\delta_{ik} - \int_r^\infty G_i^+(r') \sum_{j=1}^N W_{ij}(r')\, G_j(r')\, c_j(r')\,dr' + \int_r^\infty G_i^+(r') \sum_{j=1}^N W_{ij}(r')\, G_j^+(r')\, c_j^+(r')\,dr' , \tag{3.13a}$$

$$c_i^+(r) = \int_0^r G_i(r') \sum_{j=1}^N W_{ij}(r')\, G_j(r')\, c_j(r')\,dr' - \int_0^r G_i(r') \sum_{j=1}^N W_{ij}(r')\, G_j^+(r')\, c_j^+(r')\,dr' \tag{3.13b}$$

for $i=1,2,\ldots,N$. This scheme was proposed by Alder, Roesel, and Morf[4] and Ichimura *et al.*[5] They used a differential form of these equations.

When solving these equations iteratively, a start is made at infinity (in practice a few hundred or even thousand fm), where the $c_j(r)$ values are known, due to the boundary condition (3.11a), but the $c_j^+(r)$ are not. However, the product $G_i^+ W_{ij} G_j^+$ oscillates rapidly over the classically allowed region of the integration range which tends to nullify the contribution of the term with $c_j^+(r)$. This will also be apparent from some of the figures in the next section. It is, therefore, justifiable to take the value of these coefficients equal to zero as a first guess. Now, a first approximation to $c_i(r)$ can be generated by the inward integration of Eq. (3.13a) from infinity to r_0. The obtained values of $c_i(r)$, together with the initial condition (3.11c), are used in an outward integration of Eq. (3.13b) from r_0 to infinity, where the term with $c_i(r)$ is now considered as a known inhomogeneous function. This outward integration gives a first approximation to $c_i^+(r)$ with a value at infinity, which corresponds to a first approximation of the R-matrix elements.

The iteration procedure continues as a second inward integration of Eq. (3.13a) using the calculated values of $c_i^+(r)$ and so forth, until convergence is obtained for $c_i^+(\infty)$. In the cases tested, only a few steps in the iteration process were needed.

B. Perturbative iteration scheme

The set of coupled integral equations for the amplitudes $c_i(r)$ and $c_i^+(r)$ can also be written as

$$c_i(r) = \frac{2}{i}\delta_{ik} + \int_0^r G_i^+(r') \sum_{j=1}^N W_{ij}(r') [G_j(r')\, c_j(r') - G_j^+(r')\, c_j^+(r')] dr'$$
$$- \int_0^\infty G_i^+(r') \sum_{j=1}^N W_{ij}(r') [G_j(r')\, c_j(r') - G_j^+(r')\, c_j^+(r')] dr' , \tag{3.14a}$$

$$c_i^+(r) = \int_0^r G_i(r') \sum_{j=1}^N W_{ij}(r') [G_j(r')\, c_j(r') - G_j^+(r')\, c_j^+(r')] dr' . \tag{3.14b}$$

In this scheme, which was proposed by Raynal,[6] the coupling potential W is considered as a perturbation.

To illustrate the iteration procedure the results for the nth step of the iteration in case $k=1$ are written as

$$c_i^{(n)}(r) = \frac{2}{i}\delta_{i1} + \int_0^r G_i^+(r') X_i^{(n)}(r') dr' - \int_0^\infty G_i^+(r') X_i^{(n)}(r') dr' \tag{3.15a}$$

$$c_i^{+(n)}(r) = \int_0^r G_i(r') X_i^{(n)}(r') dr' , \tag{3.15b}$$

where

$$X_i^{(n)} = W_{i1}[G_1 c_1^{(n-1)} - G_1^+ c_1^{+(n-1)}] + \sum_{j=2}^{i-1} W_{ij}[G_j c_j^{(n)} - G_j^+ c_j^{+(n)}] + \sum_{j=i}^{N} W_{ij}[G_j c_j^{(n-1)} - G_j^+ c_j^{+(n-1)}] \tag{3.16a}$$

for $i=2,3,\ldots,N$ and

$$X_i^{(n)} = W_{11}[G_1 c_1^{(n-1)} - G_1^+ c_1^{+(n-1)}] + \sum_{j=2}^{N} W_{1j}[G_j c_j^{(n)} - G_j^+ c_j^{+(n)}] \tag{3.16b}$$

for $i=1$.

The calculation of Eq. (3.15) starts with $i=2$, using (3.16a) under the initial conditions

$$c_j^{(0)}(r_0) = \frac{2}{i}\delta_{j1}, \quad c_j^{+(0)}(r_0) = 0 . \tag{3.17}$$

This component must be integrated to infinity, due to the third term in (3.15a), before the calculation can be continued for $i=3$. The iteration step ends with the integration of the first component using (3.16b).

We have also investigated a perturbative scheme with the initial conditions

$$c_j^{(0)}(\infty) = \frac{2}{i}\delta_{j1}, \quad c_j^{+(0)}(\infty) = 0 , \tag{3.18}$$

and adapted integral expressions for $c_i^{(n)}(r)$ and $c_i^{+(n)}(r)$. However, in the cases tested, the results varied little from those obtained with the initial conditions (3.17).

To solve Eqs. (3.13) and (3.14) we use the relatively slow variation of the amplitudes $c_i(r)$ and

$c_i^+(r)$ with respect to the rapid oscillations of the functions $G_i(r)$ and $G_i^+(r)$ in the classically allowed region. This behavior is understood by noting that $c_i(r)$ and $c_i^+(r)$ nearly lose their r dependence on the midpoint of an interval. This dependence is weak as long as the difference between the true potential and the reference potential is small. Thus, a choice of step size has to be made so that small variations of $c_i(r)$ and $c_i^+(r)$ over an interval can be neglected.

Assuming that in the first iteration step we have already integrated Eq. (3.13a), for example, from the right up to r_r and using the values of $c_i(r_r)$, this equation yields a first-order contribution to $c_i(r_l)$ at the "left-hand" boundary r_l, provided integrals of the form

$$\int_{r_l}^{r_r} G_i(r)(r-\bar{r})^m G_j(r)\,dr \tag{3.19}$$

are determined. Expressing $G_i(r)$ [and also $G_i^+(r)$] in Airy functions and introducing an average value for the first derivatives [see (3.4)] when the constant α becomes independent of the channels, integrals are obtained of the form

$$\int_{r_l}^{r_r} (r-\bar{r})^m \mathrm{Ai}[\alpha(\beta_i+r)]\ \mathrm{Bi}[\alpha(\beta_j+r)]\,dr\,. \tag{3.20}$$

This type of integral can be evaluated analytically. The analytical expressions for the integrals of $m=0, 1, 2$; $\beta_i=\beta_j$ and for $m=0, 1$; $\beta_i\neq\beta_j$ were given by Gordon,[3] while the expression for $m=2$ and $\beta_i\neq\beta_j$ is given in the Appendix.

IV. RESULTS AND DISCUSSION

In this section we present results with respect to the amplitudes $c(r)$, $c^+(r)$ and the R-matrix elements for two heavy ion scattering test cases. In these cases, the multiple Coulomb excitation of the ground-state rotational band of a doubly even nucleus with the corresponding spin sequence has been considered. The reduced transition matrix elements which are used were calculated according to the simple rotational model starting from given values of the reduced $E2$ and $E4$ matrix elements, $\langle 2^+\|M(E2)\|0^+\rangle$ and $\langle 4^+\|M(E4)\|0^+\rangle$, respectively. Before starting our investigation on the heavy ion test cases, we made for a light ion test case[9] a comparison between iteratively calculated R-matrix elements and those calculted with a conventional coupled-channel computer program (AROSA[8]). It turns out that a three- to four-figure correspondence is obtained.

Multiple Coulomb excitation of ^{238}U by 385 MeV Kr. (Ref. 10)

For this case, the Sommerfeld parameter and wave number are approximately 244 and 29, respectively. The target spin sequence is $0^+, 2^+, 4^+, \ldots, 20^+$ ($N=121$). In Fig. 1 the values of the complex R-matrix element, with a set of quantum numbers and hypothetical $E2$ and $E4$ values as mentioned in the figure, are plotted with a logarithmic radial scale in the complex plane, for successive iteration steps of both schemes. This figure shows as a surprising result the very rapid convergence of the inward-outward iteration scheme when compared to the perturbative one. It is seen that the perturbative values jump from one quadrant to the other while approaching the convergence limit only after more than about thirteen steps. On the contrary, the inward-outward scheme has a starting value which already nearly coincides with the convergence limit. It appears that for larger values of the reduced $E2$ transition matrix element, the rate of convergence for the perturbative iteration scheme is poorer. For the more realistic reduced $E2$ element of 3.5 eb, it diverges. The inward-outward scheme needs only a few steps to converge in this case. Therefore, from now on we concentrate our investigation on the inward-outward iteration scheme, using an $E2$ element equal to 3.5 eb.

Figure 2 shows the behavior of the amplitudes $c(r)$ and $c^+(r)$, during the first and final iteration step, for the set of quantum numbers $I_0=0$, $I=2$, $l_0=l=100$. Numerically speaking, the fourth iteration step gives at least a three-figure agreement

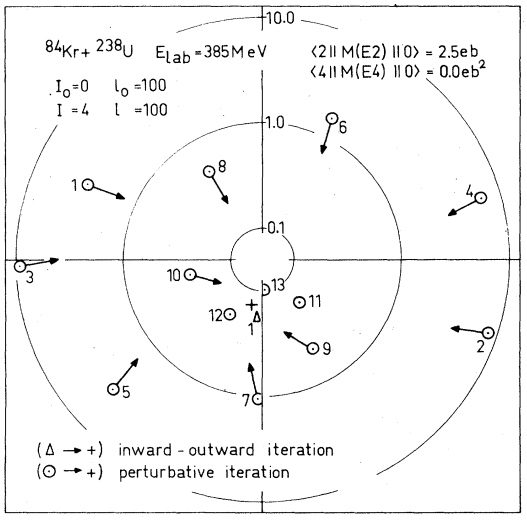

FIG. 1. A R-matrix element for a heavy ion scattering case, plotted with a logarithmic radial scale in the complex plane and calculated for successive iteration steps according to the inward-outward iteration scheme and the perturbative one. The convergence limit is indicated by a cross (+). Note the rapidity of convergence of the inward-outward scheme.

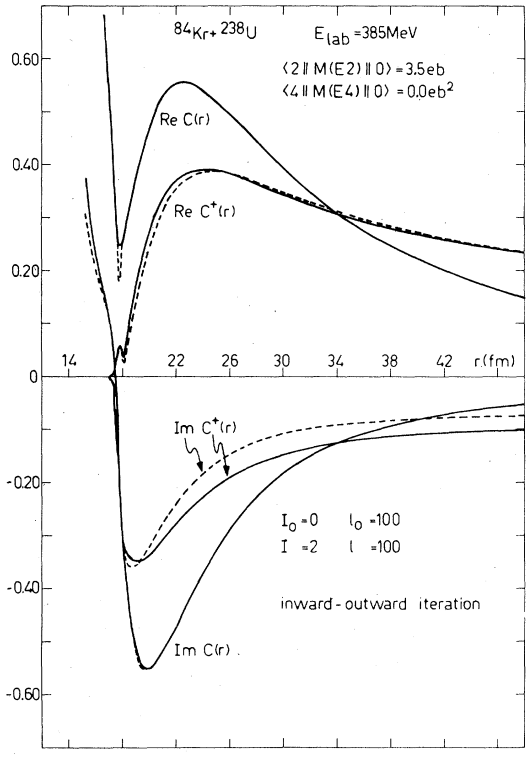

FIG. 2. This figure illustrates the inward-outward iteration scheme for a heavy ion scattering case. The amplitudes $c(r)$ and $c^+(r)$ are plotted as a function of r for the first iteration step (---) and the final one (——). The difference between the first and final iteration steps for $c(r)$ is visible only in the neighborhood of the classical turning points. The location of the latter is given in Fig. 3.

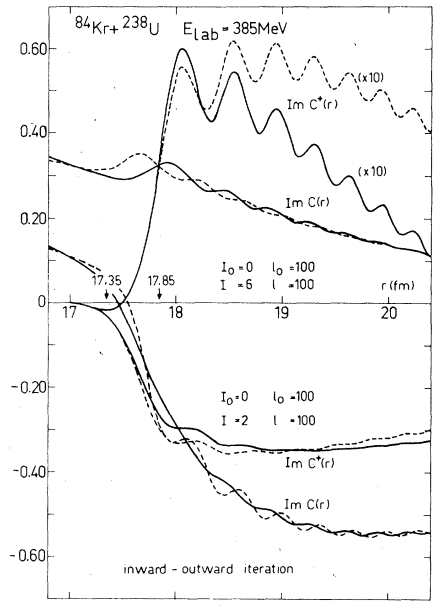

FIG. 3. The same as Fig. 2, but the imaginary parts of $c(r)$ and $c^+(r)$ are now plotted on a larger r scale for two different sets of quantum numbers. The inner- and outermost classical turning points are indicated by arrows.

with the final result. We note that the influence of $c^+(r)$, obtained in an outward integration, on $c(r)$ during the next inward integration over the classically allowed region is rather weak. Only in the region around the classical turning points of the decoupled set of equations the difference between the first and final iteration steps is visible in the figure. Clearly, even one iteration step yields a reasonable result. To study the behavior of the amplitudes in more detail, the imaginary parts of $c(r)$ and $c^+(c)$ are plotted in Fig. 3 on a larger r scale for the above-mentioned set of quantum numbers and, additionally, for $I_0=0$, $I=6$, $l_0=l=100$. Both sets, but especially the latter, suggest that the step sizes must be chosen with care over a limited part of the integration range outside the turning points, due to the tendency of the amplitudes to oscillate here. In connection with the foregoing, the general behavior of the amplitudes may be summarized as follows: They change monotonically inside the innermost turning point and tend to oscillate outside it before approaching

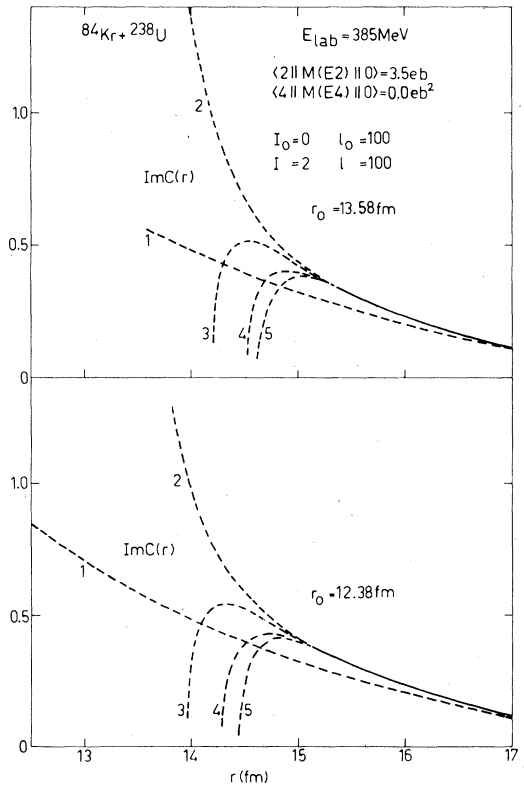

FIG. 4. This figure shows the behavior of the imaginary part of $c(r)$ for two different values of the starting point r_0, plotted as a function of r for the first part of the integration range and for successive iteration steps.

constant values in the asymptotic region.

In the previous section, it is stated that the starting point r_0 has to be taken so that its choice does not affect the value of the R-matrix elements asymptotically. It seems that, on the one hand, making r_0 too small gives rise to diverging asymptotic values of these elements, while on the other hand, for large values of r_0 the R-matrix elements become dependent on r_0. However, in the present case, the margin is rather large, as can be seen from Fig. 4. This figure shows for two different r_0 values the imaginary part of $c(r)$, which is plotted as a function of r for the first part of the integration range and for successive iteration steps. The upper part of the figure corresponds to starting values of the components $\psi_i^k(r)$ in the solution vector of about exp(−20), while the lower part corresponds to values of about exp(−30). It is seen that outside the starting point the amplitude for successive iteration steps changes very rapidly; nevertheless, it converges for both r_0 values to the same value at about 15.5 fm, far inside the innermost turning point of the decoupled set of equations. As Fig. 3 shows, this turning point is located at 17.35 fm. The behavior of $c^+(r)$ and the real part of $c(r)$ are similar. In general, such a behavior guarantees a stable iteration process, since it means that numerically speaking the components $\psi_i^k(r)$, due to (3.10b), obtain a significant value inside the innermost turning point. Comparing the R-matrix elements at infinity for the present two r_0 values, it is seen that a two- to three-figure correspondence is obtained, illustrating the degree of independence on r_0.

Also, a comparison is made with a conventional coupled-channel calculation in the sense of Sec. II. For this, only the computer program JUPIGOR[11] was available. It uses Airy functions as piecewise analytic reference solutions too. The results are presented in Table I. Comparing the significant R-matrix elements, a two- to three-figure correspondence is obtained, even for the high-spin states. Calculations of the modulus give rise to discrepancies of about one per cent. In view of the uncertainties in experimental excitation probabilities,[12] such an accuracy may be called satisfactory. Note that there is a considerable reduction of computation time. With our computer, the average computation time for one integration step when solving a system of 121 coupled equations takes about 140 sec for a conventional coupled-channel calculation; but for the inward-outward scheme it takes about 4.3 sec, including four iteration steps. Every extra iteration step takes about 0.3 sec.

Finally, it should be noted that iteration schemes based on the integral form of the Schrödinger equation, have been studied elsewhere in light particle problems for inelastic scattering as well as for rearrangement.[13] In that study, an analysis of the kernel eigenvalue problem was made in order to understand the convergence properties. In this study such an analysis was not made; however, it is believed that the striking difference in convergence properties of the two iteration schemes, examined here, has to be sought in the fact that in the inward-outward scheme, the amplitudes $c(r)$ and $c^+(r)$ are iterated independently, while this is not the case in the perturbative scheme.

Multiple Coulomb excitation of ^{238}U by 1000 MeV Pb

This case has been studied to investigate the stability of the inward-outward iteration scheme for very heavy ion multiple excitations. The Sommerfeld parameter and wave number are now 542 and 53, respectively. The target spin sequence chosen is $0^+, 2^+, 4^+, \ldots, 32^+$ ($N=289$). Figure 5 illustrates the behavior of the imaginary parts of the amplitudes $c(r)$ and $c^+(r)$ during the first and the final iteration step, for a set of quantum numbers mentioned in the figure. It turns out that in this case, too, only a few iteration steps are needed. Numerically speaking, the sixth iteration step gives at least a three-figure agreement with the final result. In this figure, the amplitudes are plotted as a function of r for the region in the neighborhood of the classical turning points, as is done in Fig. 3 for the excitation by ^{84}Kr. Comparing both figures shows a similar behavior, although the amplitudes in Fig. 5 have a slightly more oscillatory dependence on the integration variable r.

The insensitivity of the R-matrix elements to the starting point r_0 has also been investigated for the present case. This is illustrated in Fig. 6, where for two different r_0 values the imaginary part of $c(r)$ is plotted as a function of r for the first part of the integration range and for successive iteration steps. The upper and lower part of the figure correspond to starting values of the components $\psi_i^k(r)$ in the solution vector of about exp(−20) and exp(−30), respectively. It is seen that, as in Fig. 4, the amplitude converges for both r_0 values to the same value at about 19.6 fm, sufficiently inside the innermost turning point, which is located at 20.64 fm. The amplitude $c^+(r)$ and the real part of $c(r)$ show a similar behavior. This behavior guarantees a stable iteration process. The degree of independence on r_0 is illustrated by comparing asymptotically the R-matrix elements for both r_0 values. This comparison shows a two- to three-figure correspondence.

It must be noted that in a similar case to that

TABLE I. Selected $R^J_{I l; 0 l_0}$ values for $^{84}Kr + ^{238}U$ with $E_{lab} = 385$ MeV, $\langle 2 \| M(E2) \| 0 \rangle = 3.5\ eb$, $\langle 4 \| M(E4) \| 0 \rangle = 0.0\ eb^2$. The values for a quantum-mechanical coupled-channel calculation of conventional (Conv. C. C.) type (JUPIGOR), as well as the values for an inward-outward iterative (Inw.-Outw. Iter.) calculation after four iteration steps are given. The significant elements show a correspondence of about two and sometimes three figures, even for the high-spin states. The computation time per integration step, solving a system of 121 coupled equations for $I_{max} = 20$, takes about 140 sec for the former calculation, while for the latter, it takes about 4.3 sec. Left entries mean real parts, middle entries mean imaginary parts, and right entries mean the moduli. Additional exponents have been added in parentheses above the columns.

$J = l_0 = 100$

$I=0$								$l=l_0$								
							(0)	(0)	(0)							
Conv. C. C.							0.120	0.197	0.231							
Inw.-Outw. Iter.							0.119	0.195	0.229							
									0.9%							
$I=4$		$l=l_0-4$			$l=l_0-2$			$l=l_0$			$l=l_0+2$				$l=l_0+4$	
	(0)	(−1)	(0)	(0)	(−1)	(0)	(−1)	(−1)	(−1)	(−1)	(−1)	(−1)	(−1)	(0)	(0)	
Conv. C. C.	0.113	−0.560	0.126	−0.103	0.163	0.105	0.919	−0.135	0.929	−0.776	0.535	0.943	0.171	−0.117	0.118	
Inw.-Outw. Iter.	0.116	−0.533	0.127	−0.103	0.152	0.104	0.906	−0.141	0.917	−0.777	0.515	0.932	0.196	−0.118	0.119	
			0.8%			0.8%			1.3%			1.2%			1.0%	
$I=8$		$l=l_0-8$			$l=l_0-4$			$l=l_0$			$l=l_0+4$				$l=l_0+8$	
	(0)	(−1)	(0)	(−1)	(−1)	(0)	(−1)	(−1)	(−1)	(−1)	(−1)	(−1)	(−1)	(−1)	(−1)	
Conv. C. C.	0.120	0.971	0.154	0.685	0.766	0.103	0.648	0.624	0.900	0.727	0.296	0.785	0.714	−0.400	0.819	
Inw.-Outw. Iter.	0.119	0.995	0.155	0.682	0.785	0.104	0.644	0.628	0.899	0.713	0.324	0.783	0.714	−0.388	0.813	
			0.6%			1.2%			0.1%			0.3%			0.7%	
$I=12$		$l=l_0-12$			$l=l_0-6$			$l=l_0$			$l=l_0+6$				$l=l_0+12$	
	(−1)	(0)	(0)	(−1)	(−1)	(−1)	(−2)	(−1)	(−1)	(−1)	(0)	(0)	(0)	(0)	(0)	
Conv. C. C.	−0.157	0.126	0.127	0.165	−0.825	0.841	−0.713	0.895	0.898	−0.216	−0.105	0.107	0.104	0.144	0.178	
Inw.-Outw. Iter.	−0.159	0.127	0.128	0.167	−0.835	0.851	−0.765	0.903	0.906	−0.200	−0.106	0.108	0.104	0.147	0.180	
			0.7%			1.2%			0.9%			1.0%			1.2%	
$I=16$		$l=l_0-16$			$l=l_0-8$			$l=l_0$			$l=l_0+8$				$l=l_0+16$	
	(−2)	(0)	(0)	(−2)	(−1)	(−1)	(−2)	(−1)	(−1)	(−1)	(−1)	(−1)	(−1)	(−1)	(−1)	
Conv. C. C.	−0.375	−0.156	0.156	0.608	−0.836	0.838	0.190	−0.699	0.699	−0.108	−0.583	0.593	−0.364	−0.592	0.695	
Inw.-Outw. Iter.	−0.328	−0.157	0.157	0.656	−0.835	0.837	0.252	−0.700	0.701	−0.099	−0.579	0.588	−0.365	−0.600	0.702	
			0.6%			0.1%			0.3%			0.8%			1.0%	
$I=20$		$l=l_0-20$			$l=l_0-10$			$l=l_0$			$l=l_0+10$				$l=l_0+20$	
	(−2)	(−1)	(−1)	(−2)	(−1)	(−1)	(−3)	(−1)	(−1)	(−2)	(−1)	(−1)	(−2)	(−2)	(−1)	
Conv. C. C.	−0.365	0.722	0.723	0.232	−0.304	0.305	0.218	0.189	0.189	−0.224	−0.104	0.106	0.381	0.704	0.800	
Inw.Outw. Iter.	−0.337	0.721	0.722	0.231	−0.301	0.302	0.105	0.188	0.188	−0.215	−0.102	0.104	0.383	0.714	0.809	
			0.2%			1.0%			0.8%			1.9%			1.1%	

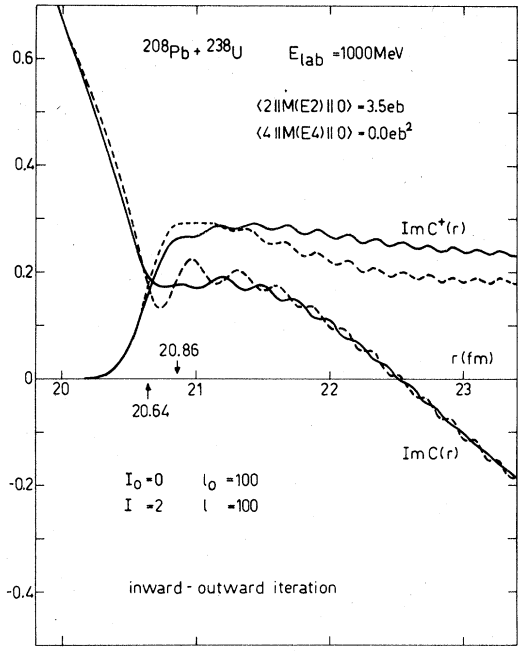

FIG. 5. This figure illustrates the inward-outward iteration scheme for a very heavy ion scattering case. The imaginary parts of the amplitudes $c(r)$ and $c^+(r)$ are plotted as a function of r for the first iteration step (---) and the final one (——). This has been done for the region in the neighborhood of the inner- and outermost classical turning points, which are indicated by arrows. The amplitudes show a slightly more oscillatory dependence on r as compared to the amplitudes in Fig. 3.

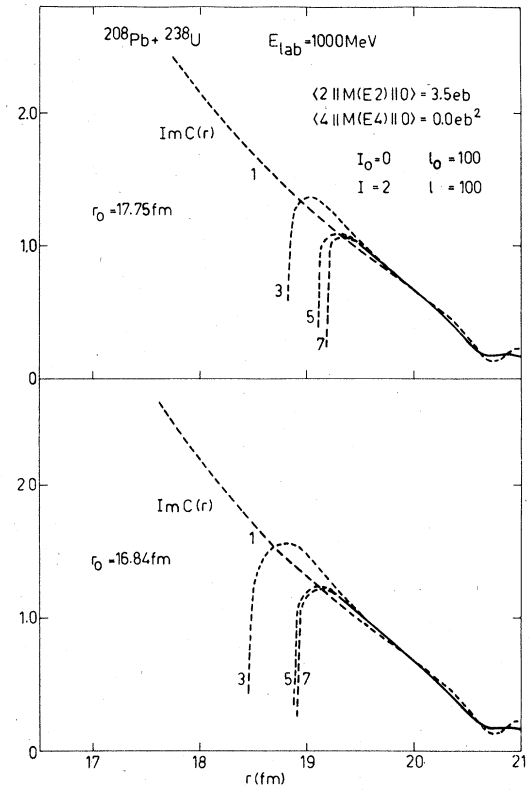

FIG. 6. This figure shows for the same very heavy ion scattering case as in Fig. 5, the behavior of the imaginary part of $c(r)$ for two different values of the starting point r_0, plotted as a function of r for the first part of the integration range and for successive iteration steps.

illustrated in Fig. 5, but with a target spin sequence of $0^+, 2^+, 4^+, \ldots, 24^+$, the inward-outward iteration scheme does not converge. Apparently, it can be considered as a further condition for a stable iteration process that the coupling scheme of the differential equations includes all experimentally relevant target states.

In conclusion, the inward-outward iteration scheme is successful and manageable even for multiple Coulomb excitation induced by very heavy ion collisions where it shows a rapid convergence.

V. COULOMB EXCITATION PROBABILITIES OF ^{84}Kr + ^{238}U at 385 MeV

To calculate the scattering amplitudes, cross sections, and excitation probabilities, use is made of some subroutines provided by the program AROSA.[8] However, it is necessary to adapt these subroutines due to the large number of J values needed in the partial-wave sums.

For the calculation of the cross sections (2.8) and excitation probabilities (2.9), a target spin sequence of $0^+, 2^+, 4^+, \ldots, 24^+$ ($N = 169$) and reduced $E2$ and $E4$ transition matrix elements equal to 3.5 eb and 0.0 eb^2, respectively, have been taken. The R-matrix elements were calculated for the following sequence: $J = 0, 40, (1)$; $42, 100, (2)$; $104, 196, (4)$; $204, 516, (8)$; $532, 1332, (16)$. The values in parentheses indicate J steps. The values of the missing R-matrix elements are obtained by interpolation.

It is well known that the number of target states, which are coupled, is reduced at high J values. To illustrate this behavior, in Fig. 7 the absolute values of some R-matrix elements are plotted against J. These values are multiplied by the weight $(2J+1)^{1/2}$, with which the R-matrix elements appear in the expression of the scattering amplitudes (2.6). It appears that the full set of coupled differential equations is necessary only up to a J value equal to about 200. For higher J values the dimension of the set can be gradually decreased.

In Figs. 8(a) and 8(b) the quantum-mechanical (QM) Coulomb excitation probabilities, calculated in the center-of-mass system, are plotted for all target states included as a function of the scattering angle θ. In addition, the probabilities are plotted from calculations based upon the semi-

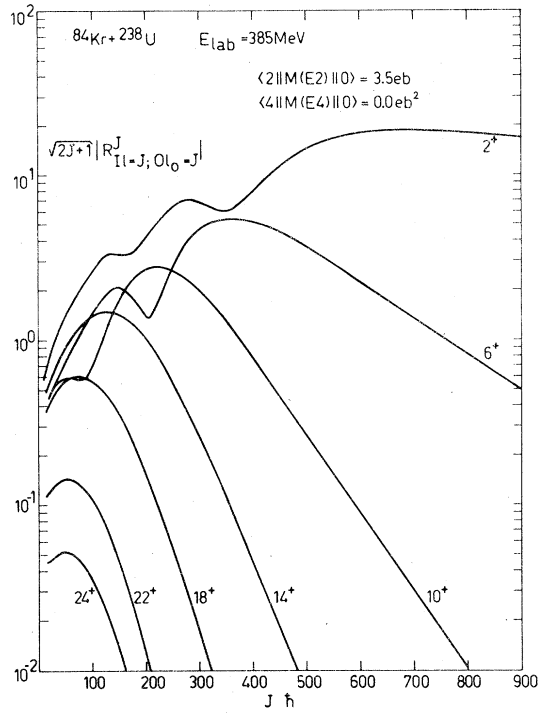

FIG. 7. The absolute values of some R-matrix elements, multiplied by a weight factor, are plotted against J for several spin states of the target.

classical (SC) theory with energy-symmetrized classical orbits.[14] Comparing both probabilities, it is seen that, as expected, the difference between the QM and SC probabilities for the low-spin states [Fig. 8(a)] is small, although significant. The difference is somewhat larger for the other states. Looking at Fig. 8(b), it is noted that at backward angles, the QM and SC probabilities for $I^\pi = 10^+$ coincide. For $I^\pi = 12^+$, 14^+, and 16^+ the QM probability becomes larger than the SC value, for $I^\pi = 18^+$ they coincide again, while for $I^\pi = 20^+$, 22^+, and 24^+ the SC probability increases relative to the QM probability. It is observed that the systematics of the differences between the QM and SC excitation probabilities, depending upon the excited target state and scattering angle, shows up quite clearly in the present study.

VI. CONCLUSIONS

The description of a heavy ion nuclear scattering process, especially of multiple Coulomb excitation, by means of a quantum-mechanical coupled-channel calculation of conventional type is not feasible at present, since the analysis involves the solution of a very large set of coupled linear second-order differential equations, which has to be solved as many times as the dimension of the set to form a full set of linearly independent solutions.

Rewriting the set of coupled differential equations in integral form, transforms it into an equivalent set of coupled first-order integral equations. Approximating the potential energy over a radial interval by a linear reference potential, makes it possible to use Airy functions as piecewise analytic reference solutions. This opens up the possibility of evaluating analytically the integrals appearing in the set of first-order integral equations. This set can be solved iteratively which, in cases of heavy ion scattering, gives a considerable reduction of computation time as compared to the above-mentioned coupled-channel calculations. The efficiency of two iteration schemes, an inward-outward and a perturbative one, was examined. It appears that for heavy ion scattering only the inward-outward scheme has practical importance, since it converges for any realistic value of the deformation parameters and needs only a few iteration steps. The accuracy which can be achieved is sufficient for practical purposes. Finally, it is concluded that the piecewise analytical approach by inward-outward iteration enables one to describe quantum-mechanically heavy ion scattering processes which are of increasing importance. Additionally, it opens up a favorable study procedure for heavy ion collisions.

ACKNOWLEDGMENTS

The author is thankful to Dr. B. J. Verhaar for helpful discussions and critical reading of the manuscript, as well as to Dr. H. J. Wollersheim from the Gesellschaft für Schwerionenforschung, Darmstadt, Germany, who performed the calculations for the excitation probabilities according to the semiclassical theory. He wishes to thank the computer center of the Eindhoven University of Technology also, where the calculations were made on a Burroughs 7700 computer.

APPENDIX

We consider integrals over Airy functions of the form

$$\int R^m A[\alpha(\beta_1+R)]\, B[\alpha(\beta_2+R)]\, dR\,,$$

where A and B are the Airy functions or any linear combinations of them. Integrals involving $m = 0, 1, 2$; $\beta_1 = \beta_2$ and $m = 0, 1$; $\beta_1 \neq \beta_2$ were given by Gordon.[3] The analytical expression for the integral with $m = 2$ and $\beta_1 \neq \beta_2$ may also be derived:

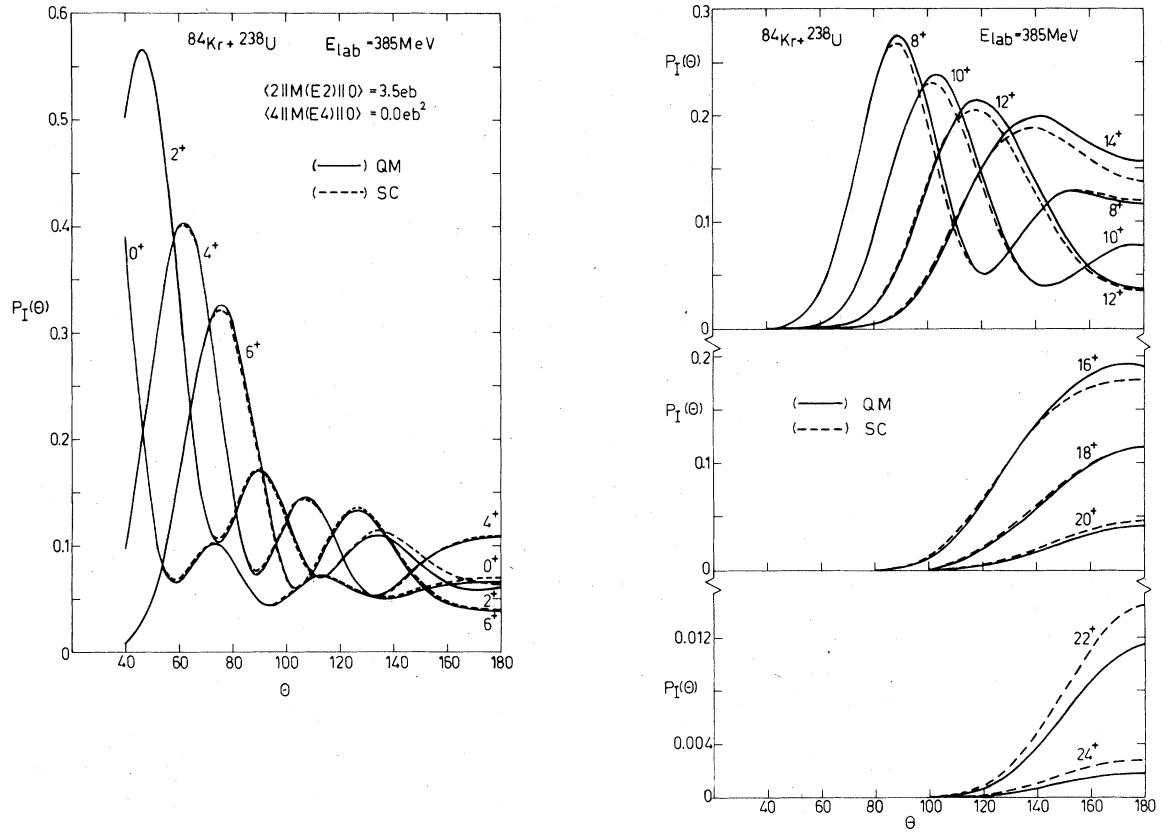

FIG. 8. (a) The quantum-mechanical (QM) and semiclassical (SC) Coulomb excitation probabilities P_I, calculated in the center-of-mass system, are plotted as a function of the scattering angle θ for the low-spin states of the target. (b) The same as (a), but the excitation probabilities P_I are now plotted as a function of the scattering angle θ for the high-spin states of the target. The difference between the QM and SC excitation probabilities depends upon both the excited target state and scattering angle.

$$\int R^2 A[\alpha(\beta_1+R)]\, B[\alpha(\beta_2+R)]\,dR$$

$$= -\frac{1}{\alpha^6(\beta_1-\beta_2)^4}\{12(\beta_1+\beta_2)+[24+2\alpha^3(\beta_1+\beta_2)(\beta_1-\beta_2)^2]R+4\alpha^3(\beta_1-\beta_2)^2R^2\}\{A[\alpha(\beta_1+R)]\, B[\alpha(\beta_2+R)]\}$$

$$+\frac{4}{\alpha^5(\beta_1-\beta_2)^3}\{\beta_2 A'[\alpha(\beta_1+R)]\, B[\alpha(\beta_2+R)]-\beta_1 A[\alpha(\beta_1+R)]\, B'[\alpha(\beta_2+R)]\}$$

$$+\frac{1}{\alpha^8(\beta_1-\beta_2)^5}\{[24+2\alpha^3(\beta_1+\beta_2)(\beta_1-\beta_2)^2]+12\alpha^3(\beta_1-\beta_2)^2R+\alpha^6(\beta_1-\beta_2)^4R^2\}$$

$$\times\{A'[\alpha(\beta_1+R)]\, B[\alpha(\beta_2+R)]-A[\alpha(\beta_1+R)]\, B'[\alpha(\beta_2+R)]\}$$

$$+\frac{4}{\alpha^7(\beta_1-\beta_2)^4}[6+\alpha^3(\beta_1-\beta_2)^2R]\{A'[\alpha(\beta_1+R)]\, B'[\alpha(\beta_2+R)]\},$$

where the prime denotes differentiation with respect to the argument. The constant β does not contain $\bar{r}$ as in (3.8).

[1]K. Alder and A. Winther, *Electromagnetic Excitation* (North-Holland, Amsterdam, 1975).
[2]J. de Boer, G. Dannhauser, H. Massmann, F. Roessel, and A. Winther, J. Phys. G 3, 889 (1977); M. W. Guidry, R. Donangelo, J. O. Rasmussen, and J. P. Boisson, Nucl. Phys. A295, 482 (1978).
[3]R. G. Gordon, J. Chem. Phys. 51, 14 (1969); R. G. Gordon, in *Methods in Computational Physics: 10, Atomic and Molecular Scattering*, edited by B. Alder, S. Fernbach, and M. Rotenberg (Academic, New York, 1971), p. 81.
[4]K. Alder, F. Roesel, and R. Morf, Nucl. Phys. A284, 145 (1977).
[5]M. Ichimura, M. Igarashi, S. Landowne, C. H. Dasso, B. S. Nilsson, R. A. Broglia, and A. Winther, Phys. Lett. 67B, 129 (1977).
[6]J. Raynal, *Computing as a Language of Physics* (IAEA, Vienna, 1972), p. 281.
[7]See Chap. IX of Ref. 1.
[8]F. Roesel, J. X. Saladin, and K. Alder, Comp. Phys. Commun. 8, 35 (1974).
[9]H. J. Wollersheim, W. Wilcke, Th.W. Elze, and D. Pelte, Phys. Lett. 48B, 323 (1974).
[10]E. Grosse, J. de Boer, R. M. Diamond, F. S. Stephens, and P. Tjøm, Phys. Rev. Lett. 35, 565 (1975).
[11]L. D. Tolsma, J. Comp. Phys. 17, 384 (1975).
[12]M. W. Guidry, E. Eichler, N. R. Johnson, G. D. O'Kelley, R. J. Sturm, and R. O. Sayer, Phys. Rev. C 12, 1937 (1975).
[13]P. J. R. Soper, Phys. Rev. C 10, 1282 (1974).
[14]A. Winther and J. de Boer, in *Coulomb Excitation*, edited by K. Alder and A. Winther (Academic, New York, 1970), p. 303.